PCCP

PAPER

View Article Online
View Journal | View Issue

Cite this: *Phys. Chem. Chem. Phys.*, 2017, **19**, 3550

Selective bond breaking of CO_2 in phase-locked two-color intense laser fields: laser field intensity dependence

Tomoyuki Endo,[ab] Hikaru Fujise,[b] Yuuna Kawachi,[b] Ayaka Ishihara,[b] Akitaka Matsuda,[b] Mizuho Fushitani,[b] Hirohiko Kono[c] and Akiyoshi Hishikawa*[ab]

Received 1st November 2016,
Accepted 26th December 2016

DOI: 10.1039/c6cp07471e

www.rsc.org/pccp

Selective bond breaking of CO_2 in phase-locked ω–2ω two-color intense laser fields (λ = 800 nm and 400 nm, total field intensity $I \sim 10^{14}$ W cm^{-2}) has been investigated by coincidence momentum imaging. The CO^+ and O^+ fragment ions produced by two-body Coulomb explosion, $CO_2^{2+} \rightarrow CO^+ + O^+$, exhibit asymmetric distributions along the laser polarization direction, showing that one of the two equivalent C–O bonds is selectively broken by the laser fields. At a field intensity higher than 2×10^{14} W cm^{-2}, the largest fragment asymmetry is observed when the relative phase ϕ between the ω and 2ω laser fields is $\sim$0 and π. On the other hand, an increase of the asymmetry and a shift of the phase providing the largest asymmetry are observed at lower field intensities. The selective bond breaking and its dependence on the laser field intensity are discussed in terms of a mechanism involving deformation of the potential energy surfaces and electron recollision in intense laser fields.

1 Introduction

Light–matter interaction in the intense field regime (field intensity $I \sim 10^{14}$ W cm^{-2}) drives a variety of interesting dynamics in molecules.[1,2] It offers unique methods to soften or harden chemical bonds[3,4] or to control the electron localization in the molecular frame[5] as demonstrated with H_2^+ (D_2^+) molecules. Since such molecular responses are determined by the property of the applied laser electric fields, intense-field coherent control is one of the most powerful approaches to manipulate photodissociation dynamics at the quantum level.

Coherent control in the intense field regime has been demonstrated with several approaches. In particular, pulse shaping techniques using a spatial phase modulator have been successfully applied to a variety of photochemical reactions, such as dissociation of $Fe(CO)_5$,[6,7] $CpFe(CO)_2Cl$,[6,8] acetophenone,[9] acetone and its derivatives,[9,10] bending of CO_2,[11] and isomerization of 1,3-cyclohexadiene[12] as well as electron localization in heteronuclear diatomic molecules.[13] Combined with the genetic algorithm, the pulse shaping techniques allow optimization of a number of parameters, such as intensity, phase, and polarization of each wavelength component, to steer the system into a target reaction pathway.

Two-color mixing is another interesting approach for the coherent reaction control, as demonstrated with various targets ranging from diatomic to polyatomic molecules.[14–20] For the two-color laser fields consisting of the fundamental (ω) and the second harmonic (2ω) fields, the laser electric field, $F(t)$, may be expressed as

$$F(t) = \bar{F}_\omega(t)\cos(\omega t) + \bar{F}_{2\omega}(t)\cos(2\omega t + \phi), \quad (1)$$

where $\bar{F}_\omega(t)$ and $\bar{F}_{2\omega}(t)$ are the temporal envelopes of the fundamental and second harmonic fields with carrier frequencies of ω and 2ω, respectively. The relative phase, ϕ, between the two laser fields determines the waveform of the laser electric fields. At ϕ = 0 or π, the amplitude exhibits the largest asymmetry between the positive and negative sides, while it becomes symmetric at $\phi = \pi/2$ or $3\pi/2$. Fig. 1(a) shows the schematic of the two-color laser electric fields at relative phases ϕ = 0, $\pi/2$, and π. Although the number of controllable laser parameters is limited, one can vary the intensity and the relative phase of the two laser fields independently (and systematically) to elucidate underlying mechanisms of coherent control, which is important for a deeper understanding and an efficient control of chemical reactions.

In the present study, we focus on the directional fragment ejection from symmetric molecules in intense laser fields. The demonstration of directional ejection control was performed with D_2^+ using few-cycle carrier-envelope-phase (CEP) locked laser pulses,[5,21] showing that the direction of deuteron ejection

[a] *Research Center for Materials Science, Nagoya University, Furo-cho, Chikusa, Nagoya, Aichi 464-8602, Japan. E-mail: hishi@chem.nagoya-u.ac.jp*
[b] *Department of Chemistry, Graduate School of Science, Nagoya University, Furo-cho, Chikusa, Nagoya, Aichi 464-8602, Japan*
[c] *Department of Chemistry, Graduate School of Science, Tohoku University, Sendai 980-8578, Japan*

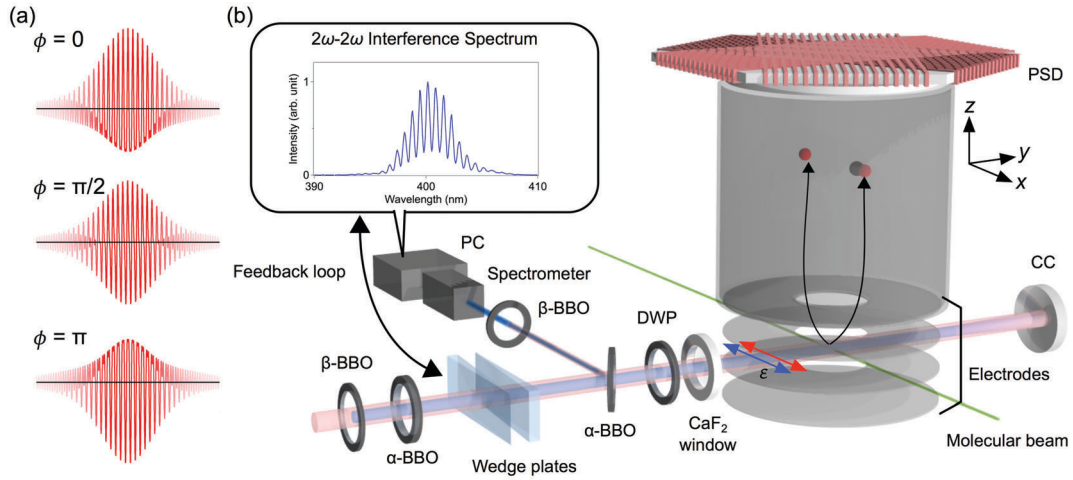

Fig. 1 (a) Schematic of the two-color laser electric fields used in the present study ($\alpha = I_{2\omega}/I_{\omega} = 0.11$), at relative phases $\phi = 0$, $\pi/2$, and π. The Gaussian functions are assumed for the envelopes, $\bar{F}_{\omega}(t)$ and $\bar{F}_{2\omega}(t)$. (b) Schematic of the experimental setup. The output of a Ti:Sapphire laser amplifier system (800 nm, 1 kHz) was introduced to a β-barium borate (BBO, type I) crystal to generate a second-harmonic pulse (400 nm). The time-delay between the fundamental (ω) and the second harmonics (2ω) was compensated by birefringent α-BBO crystals. A pair of fused silica wedges was used for fine tuning of the relative phase, which was locked by a feedback loop utilizing the $2\omega-2\omega$ interference spectrum. The polarization axis (ε) of the ω pulse was rotated to be parallel with the 2ω pulse by a dual-wavelength waveplate. DWP: dual-wavelength waveplate, CC: concave mirror, PSD: position sensitive detector.

in $D_2^+ \rightarrow D^+ + D$ varies sensitively depending on the CEP. The directional fragment ejection from D_2^+ was also demonstrated with ω–2ω laser fields,[16,19] presenting a kinetic energy dependent asymmetric fragmentation.

The coherent control of directional fragment ejection has been extended to polyatomic molecules, C_2H_2 (C_2D_2).[18,22,23] It was shown that one of the two C–H (or C–D) bonds can be selectively cleaved by CEP locked[22,23] or two-color intense laser pulses.[18] Recently, such bond breaking control has been demonstrated with CO_2 using two-color laser fields,[20] expanding the applicability of selective breaking of equivalent chemical bonds to heavier systems.

For D_2^+, the asymmetric deuteron ejection is explained by laser-induced coherent coupling of electronic states.[5,16,19,21,24] Coherent superposition of σ_g and σ_u states with an appropriate phase localizes the electron between the equivalent deuteron sites to produce D^+ ion preferentially in one direction. On the other hand, different mechanisms are proposed for acetylene, such as coherent superposition of vibrational states[22] and laser-assisted bond weakening.[23] In the former, it is proposed that a wavepacket formed by a CEP-dependent superposition of symmetric and anti-symmetric stretching vibrational states propagates on a field-free dissociative potential energy surface of acetylene dication, resulting in the directional ejection of H^+.[22]

In our previous study using two-color laser fields (pulse duration ~100 fs),[20] the Coulomb explosion of CO_2, $CO_2 \rightarrow CO_2^{2+} + 2e^- \rightarrow CO^+ + O^+ + 2e^-$, exhibits the largest fragment asymmetry at $\phi = 0$ and π, where the O^+ fragment is preferentially ejected to the larger amplitude side. The result is in good agreement with predictions by a previous theoretical study on CO_2^{2+} in intense laser fields,[25,26] suggesting that the selective bond breaking in this long pulse regime is governed by laser-induced deformation of the potential energy surface.

Since molecular responses in intense laser fields are often highly non-linear, laser field intensity is an important control parameter as demonstrated in previous studies.[27–29] Here we study the field intensity dependence of asymmetric Coulomb explosion of CO_2 for a deeper understanding of the mechanisms of selective breaking of the two equivalent C–O bonds in ω–2ω two-color intense laser fields ($I \sim 10^{14}$ W cm^{-2}).

2 Experiment

The schematic of the experimental setup is shown in Fig. 1(b). The output of a femtosecond Ti:Sapphire laser amplifier system (800 nm, 1 kHz) was introduced to an inline ω–2ω pulse generator. A β-barium borate (BBO, type I) crystal was used to generate the second harmonic (2ω) pulse from the fundamental (ω) pulse. The time-delay between the ω and 2ω pulses associated with group velocity dispersion in the ω–2ω pulse generator and the vacuum chamber window was compensated by two birefringent α-BBO crystals. A pair of fused silica wedges was used for fine-tuning of the relative phase ϕ, which was locked by a feedback loop utilizing the 2ω–2ω spectral interference.[20] The root mean square of the measured phase distribution was 0.043π (7.8°) without stabilization, which was reduced to 0.019π (3.5°) with stabilization. The long term (30 min) drift of the mean phase was also reduced from -0.010π (−1.8°) to $-6 \times 10^{-4}\pi$ (−0.1°). The polarization axis of the ω pulse was rotated to be parallel to that of the 2ω pulse by a true-zero order dual-wavelength waveplate ($\lambda/2$ for ω, λ for 2ω). The pulse durations of the ω and 2ω pulses were measured in the interaction region to be 45 fs and 110 fs, respectively. The relative phase in the interaction region was calibrated by a separate experiment measuring the energy distribution of high-order above threshold

ionization (ATI) peaks associated with the back-scattered electrons from Xe.[30] The relative phase was calibrated so as to have the maximum back-scattered electron energy at $\phi = 0.28\pi$ (50°).

Two laser pulses were collinearly focused on the molecular beam of CO_2 by a concave mirror (f = 75 mm) placed in an ultrahigh vacuum chamber (see Fig. 1(b)). The fragment ions produced by Coulomb explosion of CO_2, $CO_2 \rightarrow {CO_2}^{2+} + 2e^- \rightarrow CO^+ + O^+ + 2e^-$, in intense laser fields were accelerated by four electrodes in a velocity map configuration and detected by a position sensitive detector (PSD) for coincidence momentum imaging.[31,32] The three-dimensional momentum vector, $\mathbf{p} = (p_x, p_y, p_z)$, of respective ions was calculated from the position and the arrival time at the detector for each dissociation event.[31,32] The total kinetic energy release was defined as the sum of the kinetic energy of the fragments, $E_{\mathrm{kin}} = \sum_i |\mathbf{p}_i|^2/2m_i$, where $\mathbf{p}_i$ and m_i are the three-dimensional momentum and the mass of the i-th fragment ion, respectively. The momentum matching condition, $|\mathbf{p}_{CO^+} + \mathbf{p}_{O^+}| \leq 15$ a.u., was applied to discriminate true coincidence events (detecting the CO^+ and O^+ fragment ions from a single ${CO_2}^{2+}$ parent ion) from false events.

The laser field intensities of the ω and 2ω laser fields, I_ω and $I_{2\omega}$, in the interaction region were calibrated separately by using the ponderomotive energy shift of the ATI photoelectron peaks of Xe atoms. The photoelectron images were recorded by the same experimental setup with inverted electrode polarity. In this paper, the total laser field intensity is denoted as $I_{\omega+2\omega} = I_\omega + I_{2\omega}$, and the ratio of the ω and 2ω laser field intensity, $\alpha = I_{2\omega}/I_\omega$, is fixed to 0.11 as used in the previous study for the phase calibration.[30]

3 Results and discussion

Fig. 2 shows a coincidence momentum image of the O^+ ions for the two-body Coulomb explosion pathway, obtained by averaging over ϕ (from 0 to 2π). The total laser field intensity is $I_{\omega+2\omega} = 5.6 \times 10^{14}$ W cm^{-2} ($I_\omega = 5.1 \times 10^{14}$ W cm^{-2} and $I_{2\omega} = 5.3 \times 10^{13}$ W cm^{-2}, $\alpha = I_{2\omega}/I_\omega = 0.11$). The momentum image shows slightly asymmetric distribution along the laser polarization direction (x-axis), as observed for the one-color case,[20] due to non-uniform detector sensitivity. Contrary to the expectation from the π molecular orbital,[33,34] strong peaks are observed along the laser polarization direction as reported in a previous study using ~100 fs laser pulses.[35] In addition, a weak isotropic feature was observed in Fig. 2 forming a circular distribution in the same kinetic energy region. The former and the latter are assigned to the direct dissociation from the ground state of ${CO_2}^{2+}$ ($X^3\Sigma_g^-$) and the predissociation of the metastable excited states ($a^1\Delta_g$ and $b^1\Sigma_g^+$), respectively.[20,36,37]

To evaluate the asymmetry of fragment ions, we defined an asymmetry parameter,

$$A(\phi) = \frac{Y_+(\phi) - Y_-(\phi)}{Y_+(\phi) + Y_-(\phi)}. \quad (2)$$

Here $Y_+(\phi)$ and $Y_-(\phi)$ are the yields of the O^+ fragments from ${CO_2}^{2+}$ with positive ($p_x > 0$) and negative ($p_x < 0$) momenta along the laser polarization direction. These yields are evaluated from the coincidence events observed in the areas denoted in Fig. 2, after the detector sensitivity correction (5%). The radial range corresponds to the total kinetic energy E_{kin} between 3 eV and 10 eV. The angular range with respect to the laser polarization direction is set between −45° and 45° to reduce the contributions from the metastable components.

Fig. 3 shows the asymmetry parameters recorded as a function of the relative phase ϕ at two different total laser field intensities. At a total field intensity of $I_{\omega+2\omega} = 5.6 \times 10^{14}$ W cm^{-2}, the asymmetry parameter $A(\phi)$ exhibits a clear oscillatory behavior with its maximum and minimum at $\phi \simeq 0$ and π,[20] respectively. On the other hand, at a reduced total field intensity of $I_{\omega+2\omega} = 0.76 \times 10^{14}$ W cm^{-2} ($I_\omega = 6.9 \times 10^{13}$ W cm^{-2} and $I_{2\omega} = 7.3 \times 10^{12}$ W cm^{-2}), the oscillation amplitude increases from 0.04 to 0.07. In addition, a positive shift of the phase was observed. These results suggest that different mechanisms are involved in

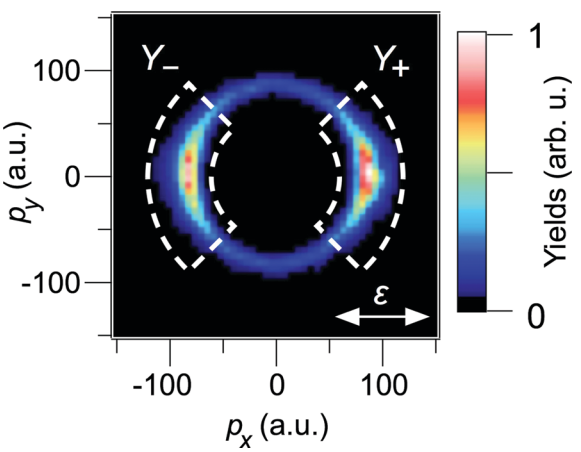

Fig. 2 The phase-averaged coincidence momentum image of the O^+ fragments in the p_x–p_y plane with the vertical momentum $|p_z| \leq 5$ a.u. obtained for the Coulomb explosion of $CO_2 \rightarrow {CO_2}^{2+} + 2e^- \rightarrow CO^+ + O^+ + 2e^-$ in two-color intense laser fields (800 nm and 400 nm, $I_{\omega+2\omega} = 5.6 \times 10^{14}$ W cm^{-2}). The momentum areas used to evaluate the ion yields, Y_+ and Y_-, are indicated by dashed line. ε denotes the laser polarization direction.

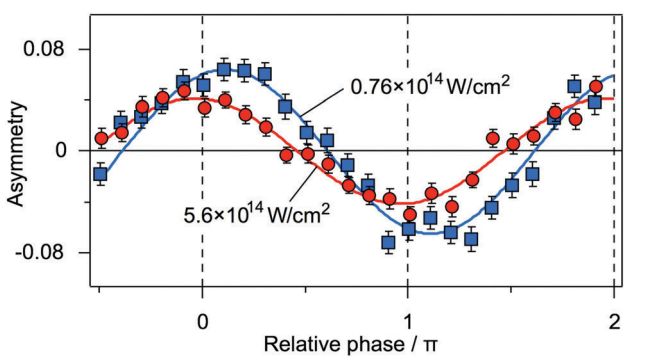

Fig. 3 Asymmetry parameters of the O^+ fragment ions at two different total laser field intensities, $I_{\omega+2\omega} = 5.6 \times 10^{14}$ W cm^{-2} (red circle) and 0.76×10^{14} W cm^{-2} (blue square). Solid lines are numerical fits by a cosine function.

the selective breaking of equivalent bonds of CO_2 depending on the laser field intensity.

Laser field intensity dependence of the directional ejection of fragment ions has been discussed with several molecules, D_2^+,[27] DCl^+,[28] HOD[38] and toluene[39] in CEP-locked intense laser fields, which show a decrease in the asymmetry with increasing field intensity, as observed in the present study. For an asymmetric molecule DCl^+,[28] the decrease in the asymmetry is interpreted in terms of molecular tunneling ionization rates, which become less sensitive to the molecular orientation as the field intensity increases. For a symmetric molecule D_2^+,[27] on the other hand, it is attributed to the increase in the range of the initial phase for the coherent coupling. As the laser field intensity increases, the time range for the recollision excitation to occur within an optical cycle becomes broader, which results in a reduced visibility of quantum interference between g and u states or a decrease in the fragment asymmetry. However, quantum interference may not be the dominant mechanism of the selective bond breaking of CO_2 because many excited states could be involved in the dissociation process.[39] Indeed, unlike D_2^+,[27] the asymmetry parameter shows no clear dependence on the total kinetic energy E_{kin} in the field intensity range investigated in the present study (not shown, see Fig. 4(c) in ref. 20).

To clarify the origin of the field intensity dependence, we measured the phase dependence of the asymmetry parameter at various total intensities, $I_{\omega+2\omega}$, ranging from 0.54×10^{14} W cm^{-2} to 5.6×10^{14} W cm^{-2} with the fixed intensity ratio ($\alpha = 0.11$). The asymmetry parameters are analyzed at each intensity by a least-squares fitting to a cosine function of ϕ,

$$A(\phi) = A_0 \cos(\phi - \phi_0), \quad (3)$$

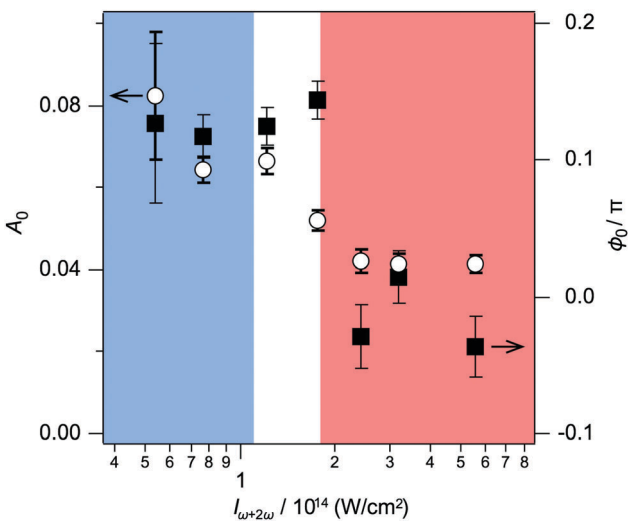

Fig. 4 Obtained fitting coefficients A_0 (circle) and φ_0 (square) of asymmetry parameters as a function of the total laser field intensity, $I_{\omega+2\omega}$. Note that the ratio of the fundamental and second harmonic field intensity $\alpha = I_{2\omega}/I_\omega$ is fixed to 0.11. Colored areas correspond to the intensity of sequential (blue, $I_{\omega+2\omega} < 1.1 \times 10^{14}$ W cm^{-2}) and non-sequential (red, $I_{\omega+2\omega} > 1.8 \times 10^{14}$ W cm^{-2}) double ionization of CO_2 in two-color laser fields (see the text for the details).

where the amplitude A_0 and the relative phase providing the maximum asymmetry ϕ_0 are adopted as fitting parameters. It should be noted that, with $\phi_0 = 0$, the O^+ fragments are preferentially ejected on the larger electric field side of the ω–2ω two-color laser pulses, while $\phi_0 = \pi$ corresponds to the ejection of O^+ on the smaller electric field side.

Fig. 4 shows the obtained parameters A_0 and ϕ_0 as a function of the total field intensity. The amplitude A_0 remains almost constant ($\sim$0.04) against an intensity decrease from $I_{\omega+2\omega} = 5.6 \times 10^{14}$ W cm^{-2} to 2×10^{14} W cm^{-2}, but shows a clear increase to $A_0 \sim 0.07$ at $I_{\omega+2\omega} = 1$–2×10^{14} W cm^{-2}. A step-like feature is observed also for the phase ϕ_0 in the same intensity range. In order to understand this characteristic behavior, we examine the electron recollision process in linearly polarized ω–2ω laser fields. Electron recollision can be decomposed to the following steps based on the three-step model:[40] (i) generation of a free electron by tunneling ionization, (ii) electron acceleration by alternating laser electric fields and (iii) electron recollision. Here, we calculated the kinetic energy of recolliding electrons, E_{elec}, by solving one-dimensional classical equations of motion along the laser polarization direction. The envelopes of two laser electric fields are assumed to be constant over time, $\bar{F}_\omega(t) = F_\omega$ and $\bar{F}_{2\omega}(t) = F_{2\omega}$ in eqn (1), and the ratio of the two electric fields is fixed at 0.33 (corresponding to $\alpha = I_{2\omega}/I_\omega = 0.11$).

Fig. 5(a)–(e) show the ω–2ω laser electric field for $I_{\omega+2\omega} = 1.39 \times 10^{14}$ W cm^{-2} ($I_\omega = 1.25 \times 10^{14}$ W cm^{-2} and $I_{2\omega} = 1.36 \times 10^{13}$ W cm^{-2}, $\alpha = 0.11$) as a function of time, $F(t)$, for selected relative phases $\phi = 0$, $\pi/4$, $\pi/2$, $3\pi/4$, and π, respectively. Also plotted is the recollision energy of electrons (born at t). The recollision energy exhibits two peaks within a cycle. Fig. 5(f) shows how these peak recollision energies depend on the relative phase. They vary in the range between 19 eV and 30 eV, corresponding to $2.5U_p(\omega)$ and $4.0U_p(\omega)$ with the ponderomotive energy of the fundamental laser field $U_p(\omega) = 7.6$ eV at $I_\omega = 1.25 \times 10^{14}$ W cm^{-2}. These upper and lower bounds of the peak recollision energy scales linearly with the total field intensity $I_{\omega+2\omega}$ as long as the field intensity ratio is fixed to $\alpha = I_{2\omega}/I_\omega = 0.11$. Since the ionization potential of CO_2^+ is I_p (CO_2^+) = 23.6 eV, non-sequential ionization from the ground state of CO_2^+ to CO_2^{2+} by electron recollision can occur at a limited phase range at this total field intensity.

For $I_{\omega+2\omega} > 1.8 \times 10^{14}$ W cm^{-2}, the recollision energy exceeds the ionization threshold of CO_2^+ at all relative phases ($2.5U_p(\omega) > I_p(CO_2^+)$), while the recollision energy is below the threshold irrespective of the phase for $I_{\omega+2\omega} < 1.1 \times 10^{14}$ W cm^{-2} ($4.0U_p(\omega) < I_p(CO_2^+)$). The intensity gap between these two regimes agrees with the intensity range where the shifts in the asymmetry amplitude, A_0, and the phase, ϕ_0, are observed in Fig. 4. This finding suggests that the recollision process is responsible for the changes in the control mechanism.

Now we discuss the mechanisms of the selective C–O bond breaking and the dependence on the laser field intensity. In the high field region ($I_{\omega+2\omega} > 1.8 \times 10^{14}$ W cm^{-2}), CO_2^{2+} is directly populated by electron recollision to undergo the interaction with the laser fields. Sato *et al.*[25,26] treated the dynamics of the structural deformation of CO_2^{2+} in two-color intense laser fields

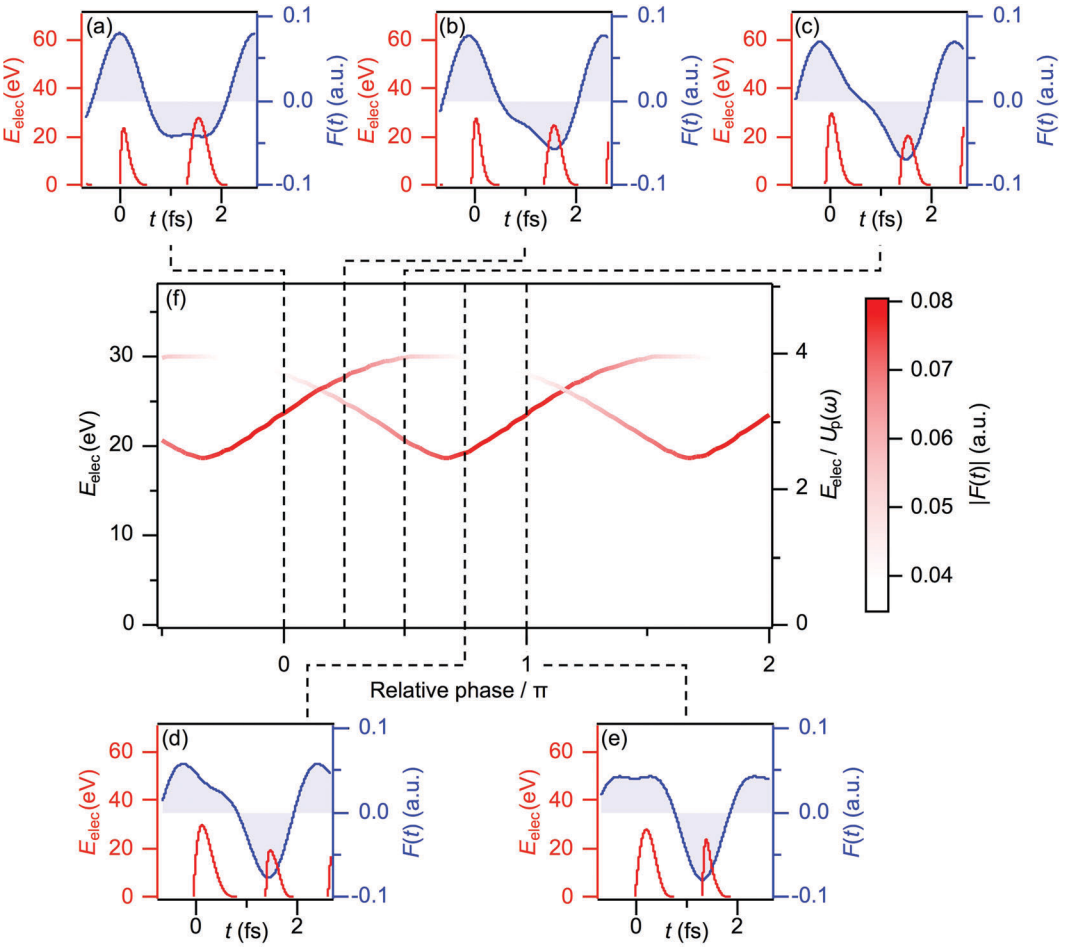

Fig. 5 The two-color laser electric fields as a function of time, $F(t)$, (blue) and the recollision energy E_{elec} of electrons born at t (red), for (a) $\varphi = 0$, (b) $\pi/4$, (c) $\pi/2$, (d) $3\pi/4$, and (e) π, respectively. (f) Relative phase dependences of two peaks observed in the recollision energy within a cycle. The color intensity corresponds to the field amplitude at the ionizing time. The intensities of the fundamental and second harmonic electric fields are 1.25×10^{14} W cm^{-2} and 1.36×10^{13} W cm^{-2}, respectively. This fundamental laser intensity, I_ω, corresponds to a threshold intensity of non-sequential double ionization of CO_2 by electron recollision in one-color intense laser fields. The ratio of two laser field intensities is fixed to $\alpha = I_{2\omega}/I_\omega = 0.11$. The ponderomotive energy of the fundamental laser fields is $U_p(\omega) = 7.6$ eV.

by using the time-dependent adiabatic state approach, where the electronic Hamiltonian including the interaction with the instantaneous laser electric field is solved by quantum chemical methods. Averaged over optical cycles, the ground-state potential energy surface of CO_2^{2+} is deformed asymmetrically along the two C–O stretching coordinates. Since the asymmetric potential deformation is attributed mainly to the non-zero cycle-averaged cubic-electric field $\langle F^3(t)\rangle$ of the two-color laser field, the largest asymmetry of the potential energy surface is expected at $\phi = 0$ and π when $\langle F^3(t)\rangle$ is maximized, showing that selective breaking of one of the two equivalent C–O bonds is expected at these relative phases. Wavepacket calculations on the deformed potential show that the dissociation of CO_2^{2+} proceeds more preferentially along one of the C–O bonds than the other, with O^+ being preferentially ejected in the larger electric field side. This is in good agreement with the observed phase relation $\phi_0 = 0$ at high field intensities ($I_{\omega+2\omega} > 1.8 \times 10^{14}$ W cm^{-2}).

On the other hand, in the case of $I_{\omega+2\omega} < 1.1 \times 10^{14}$ W cm^{-2}, the electron recollision energy is not large enough to ionize CO_2^+. The asymmetric fragmentation in this intensity range can be explained by recollision induced excitation with subsequent ionization (RESI). In this process, singly charged excited states populated by electron recollision are ionized to the doubly charged states by subsequent interaction with the laser fields.[18,41–43] Since electronically excited states have diffuse wavefunctions in general, excited molecules are more sensitive to the parameters of applied laser fields than those in the tightly bound ground states. Indeed, our previous study shows that the fragments from the excited states of CO_2^{2+} exhibit larger amplitudes in the anisotropy than those from the ground state of CO_2^{2+}.[20] This suggests that the potential energy surfaces of the recollisionally excited states of CO_2^+ could be distorted more significantly than that of the ground state of CO_2^{2+} (as long as the excited electron is involved in the bonding). Since the subsequent ionization transfers the nuclear dynamics in excited CO_2^+ to CO_2^{2+}, the fragment asymmetry in this intensity range is expected to be larger than the case of direct ionization of CO_2^{2+}, as observed experimentally. It should be noted that the recollision excitation

to CO_2^{+*} can occur above the intensity threshold for the non-sequential double ionization. The RESI mechanism would therefore contribute to the weak dependence of the A_0 parameter on the laser field intensity above 1.8×10^{14} W cm^{-2} (see Fig. 4).

The RESI mechanism also facilitates interpretation of the positive phase shift (ϕ_0 = +0.1π) observed in this intensity range. As shown in Fig. 5, the kinetic energy of the recolliding electron is sensitive to the relative phase. The maximum kinetic energy increases as ϕ increases from −0.34π to 0.54π. This indicates that recollision excitation to the excited states of CO_2^+ is more efficient for a positive phase than ϕ = 0. The competition between the deformation of the potential energy surfaces favoring a phase ϕ = 0 (or π) and the recollision excitation favoring a positive ϕ should determine the phase that provides the maximum asymmetry. This suggests that the deformation of the potential energy surfaces of the excited states of CO_2^+ in two-color intense laser fields plays an important role in the selective bond breaking of CO_2 in the low field region.

Alternatively, the asymmetric fragmentation from CO_2^{2+} at $I_{\omega+2\omega} < 1.1 \times 10^{14}$ W cm^{-2} may be interpreted in terms of sequential double ionization *via* CO_2^+. If one of the C–O bonds stretches by the interaction with the laser fields to $(OC–O)^+$, the tunneling ionization to CO_2^{2+} becomes dependent on the molecular orientation as observed for asymmetric molecules.[28] If laser electric fields directing from OC to O favor the ionization, for example by electron localization[44–46] in the up-field O site, the fragment produced by subsequent Coulomb explosion should show positive and negative asymmetry parameters at ϕ = 0 and π, respectively, as observed in the present experiments. For a deeper understanding of the control mechanism, experiments at longer wavelength[19] would be useful.

4 Summary

In the present study, we investigated selective bond breaking of CO_2 in Coulomb explosion from the doubly charged states, $CO_2 \rightarrow CO_2^{2+} + 2e^- \rightarrow CO^+ + O^+ + 2e^-$, in phase-locked two-color intense laser fields (800 nm and 400 nm, $\sim 10^{14}$ W cm^{-2}) by coincidence momentum imaging. Clear intensity dependences of the amplitude and the phase of the asymmetry parameter were observed, exhibiting a step-like features at $I_{\omega+2\omega}$ = 1–2 × 10^{14} W cm^{-2}. The selective breaking of the two equivalent C–O bonds and the intensity dependences are interpreted in the following way. For $I_{\omega+2\omega} > 1.8 \times 10^{14}$ W cm^{-2}, CO_2^{2+} formed directly by electron recollision undergoes selective breaking of two equivalent C–O bonds due to the deformation of potential energy surfaces. Below the recollision double ionization threshold ($I_{\omega+2\omega} < 1.1 \times 10^{14}$ W cm^{-2}), we proposed recollision excitation followed by the potential deformation of excited CO_2^+, which can explain both the increase of the asymmetry and the phase shift observed in the present study. The mechanisms discussed in the present study are broadly applicable to other systems in intense laser fields with relatively long pulse duration thus providing prospects for intense-field coherent reaction control.

Acknowledgements

The authors are grateful to Yukio Sato for his theoretical contributions to the discussion on the asymmetric bond breaking mechanism of CO_2^{2+}. The present study is partly supported by JSPS KAKENHI Grant Numbers 24245001, 24350006, 1632215, 16H04029, 16H04091 and by JSPS Program for Advancing Strategic International Networks to Accelerate the Circulation of Talented Researchers. T. E. acknowledges Grant-in-Aid for JSPS fellows (25·2966).

References

1 J. H. Posthumus, *Rep. Prog. Phys.*, 2004, **67**, 623.
2 F. Krausz and M. Ivanov, *Rev. Mod. Phys.*, 2009, **81**, 163.
3 P. H. Bucksbaum, A. Zavriyev, H. G. Muller and D. W. Schumacher, *Phys. Rev. Lett.*, 1990, **64**, 1883.
4 A. Zavriyev, P. H. Bucksbaum, J. Squier and F. Saline, *Phys. Rev. Lett.*, 1993, **70**, 1077.
5 M. F. Kling, C. Siedschlag, A. J. Verhoef, J. I. Khan, M. Schultze, T. Uphues, Y. Ni, M. Uiberacker, M. Drescher, F. Krausz and M. J. J. Vrakking, *Science*, 2006, **312**, 246.
6 A. Assion, T. Baumert, M. Bergt, T. Brixner, B. Kiefer, V. Seyfried, M. Strehle and G. Gerber, *Science*, 1998, **282**, 919.
7 M. Bergt, T. Brixner, B. Kiefer, M. Strehle and G. Gerber, *J. Phys. Chem. A*, 1999, **103**, 10381.
8 T. Brixner, B. Kiefer and G. Gerber, *Chem. Phys.*, 2001, **267**, 241.
9 R. J. Levis, G. M. Menkir and H. Rabitz, *Science*, 2001, **292**, 709.
10 D. Cardoza, M. Baertschy and T. Weinacht, *Chem. Phys. Lett.*, 2005, **411**, 311.
11 G. Y. Chen, Z. W. Wang and W. T. Hill III, *Phys. Rev. A: At., Mol., Opt. Phys.*, 2009, **79**, 011401.
12 M. Kotur, T. Weinacht, B. J. Pearson and S. Matsika, *J. Chem. Phys.*, 2009, **130**, 134311.
13 E. Wells, M. Todt, B. Jochim, N. Gregerson, R. Averin, N. G. Wells, N. L. Smolnisky, N. Jastram, J. McKenna, A. M. Sayler, N. G. Johnson, M. Zohrabi, B. Gaire, K. D. Carnes and I. Ben-Itzhak, *Phys. Rev. A: At., Mol., Opt. Phys.*, 2009, **80**, 063402.
14 B. Sheehy, B. Walker and L. F. DiMauro, *Phys. Rev. Lett.*, 1995, **74**, 4799.
15 H. Ohmura, N. Saito and M. Tachiya, *Phys. Rev. Lett.*, 2006, **96**, 173001.
16 D. Ray, F. He, S. De, W. Cao, H. Mashiko, P. Ranitovic, K. P. Singh, I. Znakovskaya, U. Thumm, G. G. Paulus, M. F. Kling, I. V. Litvinyuk and C. L. Cocke, *Phys. Rev. Lett.*, 2009, **103**, 223201.
17 K. J. Betsch, D. W. Pinkham and R. R. Jones, *Phys. Rev. Lett.*, 2010, **105**, 223002.
18 Q. Song, X. Gong, Q. Ji, K. Lin, H. Pan, J. Ding, H. Zeng and J. Wu, *J. Phys. B: At., Mol. Opt. Phys.*, 2015, **48**, 094007.
19 V. Wanie, H. Ibrahim, S. Beaulieu, N. Thiré, B. E. Schmidt, Y. Deng, A. S. Alnaser, I. V. Litvinyuk, X.-M. Tong and F. Légaré, *J. Phys. B: At., Mol. Opt. Phys.*, 2016, **49**, 025601.

20 T. Endo, H. Fujise, A. Matsuda, M. Fushitani, H. Kono and A. Hishikawa, *J. Electron Spectrosc. Relat. Phenom.*, 2016, **207**, 50.
21 I. Znakovskaya, P. von den Hoff, G. Marcus, S. Zherebtsov, B. Bergues, X. Gu, Y. Deng, M. J. J. Vrakking, R. Kienberger, F. Krausz, R. de Vivie-Riedle and M. F. Kling, *Phys. Rev. Lett.*, 2012, **108**, 063002.
22 A. S. Alnaser, M. Kübel, R. Siemering, B. Bergues, N. G. Kling, K. J. Betsch, Y. Deng, J. Schmidt, Z. A. Alahmed, A. M. Azzeer, J. Ullrich, I. Ben-Itzhak, R. Moshammer, U. Kleineberg, F. Krausz, R. de Vivie-Riedle and M. F. Kling, *Nat. Commun.*, 2014, **5**, 3800.
23 S. Miura, T. Ando, K. Ootaka, A. Iwasaki, H. Xu, T. Okino, K. Yamanouchi, D. Hoff, T. Rathje, G. G. Paulus, M. Kitzler, A. Baltuška, G. Sansone and M. Nisoli, *Chem. Phys. Lett.*, 2014, **595-596**, 61.
24 V. Roudnev and B. D. Esry, *Phys. Rev. Lett.*, 2007, **99**, 220406.
25 Y. Sato, H. Kono, S. Koseki and Y. Fujimura, *J. Am. Chem. Soc.*, 2003, **125**, 8019.
26 H. Kono, Y. Sato, M. Kanno, K. Nakai and T. Kato, *Bull. Chem. Soc. Jpn.*, 2006, **79**, 196.
27 H. Li, A. S. Alnaser, X.-M. Tong, K. J. Betsch, M. Kübel, T. Pischke, B. Förg, J. Schötz, F. Süßmann, S. Zherebtsov, B. Bergues, A. Kessel, S. A. Trushin, A. M. Azzeer and M. F. Kling, *J. Phys. B: At., Mol. Opt. Phys.*, 2014, **47**, 124020.
28 H. Li, X.-M. Tong, N. Schirmel, G. Urbasch, K. J. Betsch, S. Zherebtsov, F. Süßmann, A. Kessel, S. A. Trushin, G. G. Paulus, K.-M. Weitzel and M. F. Kling, *J. Phys. B: At., Mol. Opt. Phys.*, 2016, **49**, 015601.
29 D. Geißler, P. Marquetand, J. González-Vázquez, L. González, T. Rozgonyi and T. Weinacht, *J. Phys. Chem. A*, 2012, **116**, 11434.
30 D. Ray, Z. Chen, S. De, W. Cao, I. V. Litvinyuk, A. T. Le, C. D. Lin, M. F. Kling and C. L. Cocke, *Phys. Rev. A: At., Mol., Opt. Phys.*, 2011, **83**, 013410.
31 H. Hasegawa, A. Hishikawa and K. Yamanouchi, *Chem. Phys. Lett.*, 2001, **349**, 57.
32 A. Hishikawa, E. J. Takahashi and A. Matsuda, *Phys. Rev. Lett.*, 2006, **97**, 243002.
33 A. S. Alnaser, S. Voss, X.-M. Tong, C. M. Maharjan, P. Ranitovic, B. Ulrich, T. Osipov, B. Shan, Z. Chang and C. L. Cocke, *Phys. Rev. Lett.*, 2004, **93**, 113003.
34 T. Endo, A. Matsuda, M. Fushitani, T. Yasuike, O. I. Tolstikhin, T. Morishita and A. Hishikawa, *Phys. Rev. Lett.*, 2016, **116**, 163002.
35 A. Hishikawa, A. Iwamae and K. Yamanouchi, *Phys. Rev. Lett.*, 1999, **83**, 1127.
36 M. Alagia, P. Candori, S. Falcinelli, M. Lavollée, F. Pirani, R. Richter, S. Stranges and F. Vecchiocattivi, *Phys. Chem. Chem. Phys.*, 2010, **12**, 5389.
37 D. Zhang, B.-Z. Chen, M.-B. Huang, Q. Meng and Z. Tian, *J. Chem. Phys.*, 2013, **139**, 174305.
38 D. Mathur, K. Dota, D. Dey, A. K. Tiwari, J. A. Dharmadhikari, A. K. Dharmadhikari, S. De and P. Vasa, *J. Chem. Phys.*, 2015, **143**, 244310.
39 H. Li, N. G. Kling, B. Förg, J. Stierle, A. Kessel, S. A. Trushin, M. F. Kling and S. Kaziannis, *Struct. Dyn.*, 2016, **3**, 043206.
40 P. B. Corkum, *Phys. Rev. Lett.*, 1993, **71**, 1994.
41 B. Feuerstein, R. Moshammer, D. Fischer, A. Dorn, C. D. Schröter, J. Deipenwisch, J. R. Crespo Lopez-Urrutia, C. Höhr, P. Neumayer, J. Ullrich, H. Rottke, C. Trump, M. Wittmann, G. Korn and W. Sandner, *Phys. Rev. Lett.*, 2001, **87**, 043003.
42 Y. Liu, D. Ye, J. Liu, A. Rudenko, S. Tschuch, M. Dürr, M. Siegel, U. Morgner, Q. Gong, R. Moshammer and J. Ullrich, *Phys. Rev. Lett.*, 2010, **104**, 173002.
43 X. Xie, K. Doblhoff-Dier, S. Roither, M. S. Schöffler, D. Kartashov, H. Xu, T. Rathje, G. G. Paulus, A. Baltuška, S. Gräfe and M. Kitzler, *Phys. Rev. Lett.*, 2012, **109**, 243001.
44 I. Bocharova, R. Karimi, E. F. Penka, J.-P. Brichta, P. Lassonde, X. Fu, J.-C. Kieffer, A. D. Bandrauk, I. Litvinyuk, J. Sanderson and F. Légaré, *Phys. Rev. Lett.*, 2011, **107**, 063201.
45 J. Wu, M. Meckel, L. P. H. Schmidt, M. Kunitski, S. Voss, H. Sann, H. Kim, T. Jahnke, A. Czasch and R. Dörner, *Nat. Commun.*, 2013, **3**, 1113.
46 X. Gong, Q. Song, Q. Ji, H. Pan, J. Ding, J. Wu and H. Zeng, *Phys. Rev. Lett.*, 2014, **112**, 243001.